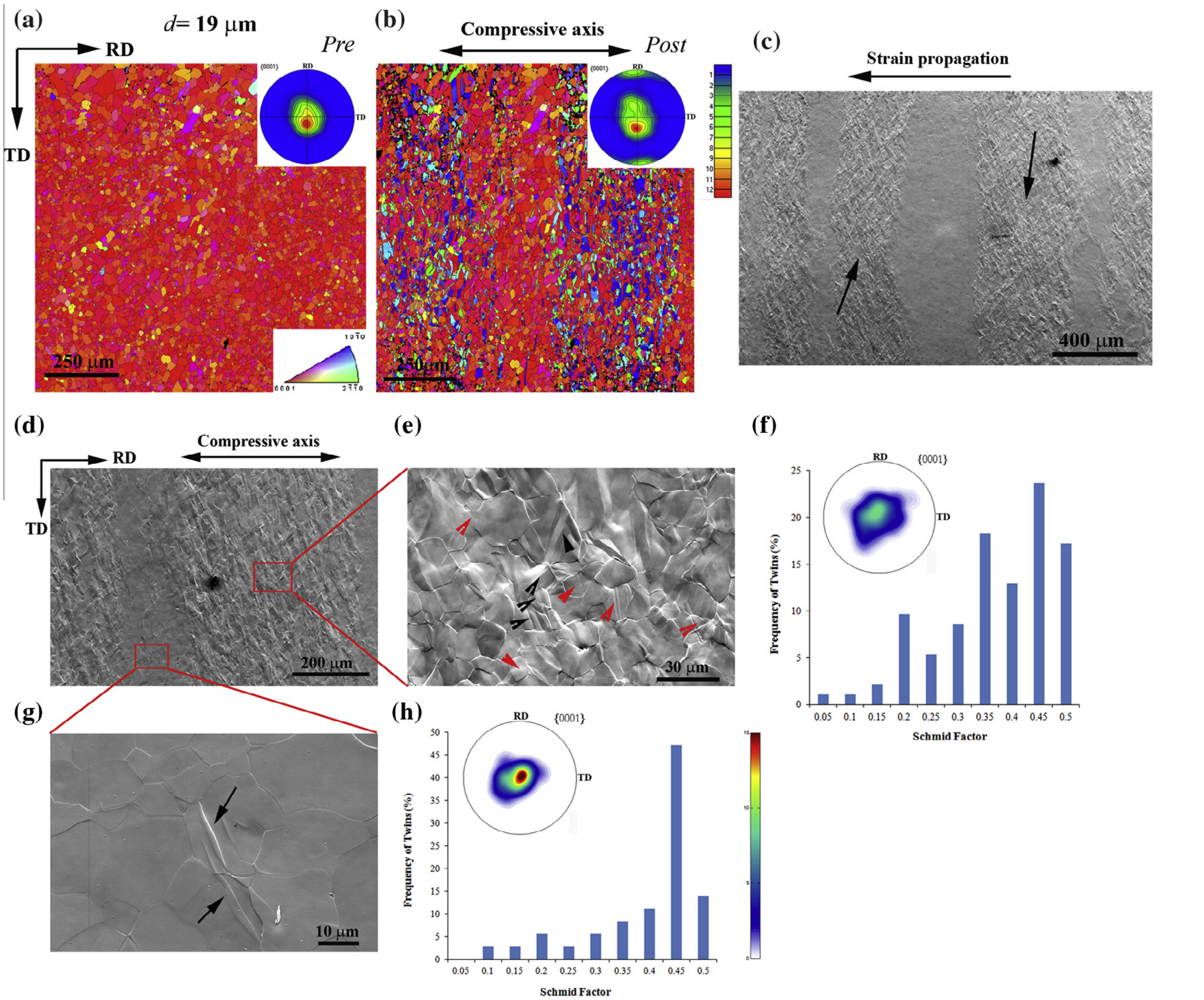

Fig. 2. (a and b) EBSD IPF maps in the ND and {0001} pole figures corresponding to the polycrystal with $d = 19$ μm (a) before testing and (b) after a strain of ~10% at 50 °C and 10^{-3} s^{-1}. (c and d) SEM micrographs showing the presence of highly twinned bands; (e and f) detailed characterization of twinning within the twin bands: (e) high magnification SEM micrograph and (f) $SF_{twinning}$ distribution and {0001} pole figure illustrating the *c*-axis corresponding to the twinned grains; (g and h) detailed characterization of incipient twinning outside the twin bands: (g) high magnification SEM micrograph and (h) $SF_{twinning}$ distribution of the twinned grains and the corresponding{0001} pole figure.

corresponding to areas within the bands (Fig. 2f) reveals that twinning took place in grains with both high and low SF, confirming that a significant fraction of twins was not activated in response to the applied stress but as a result of the need to accommodate GB stresses. Outside the Lüders bands (Fig. 2g) the few twins observed were mostly detected in grains with high SF in response to the applied stress (Fig. 2h). Altogether, the above observations confirm that, in the polycrystal with $d = 19$ μm, twinning is the dominant deformation mechanism following yielding at 50 °C and 10^{-3} s^{-1}. Twinning takes place along bands as a response to the applied stress, first in grains with high SF. Subsequently, GB stresses emerging from twin-GB interactions are released by further twinning in grains with lower SF [1,5,47] and by slip.

Fig. 3a and b illustrates the EBSD IPF maps in the ND as well as the {0001} pole figures corresponding to the deformed gage of the polycrystal with $d = 5$ μm before testing as well as after compression along RD at 50 °C and 10^{-3} s^{-1}. Again, in the as-processed condition, this polycrystal exhibits a strong basal texture, with a maximum intensity of ~12 times random (Fig. 3a) [38]. After straining a very weak maximum appears close to RD in the {0001} pole figure. Indeed, the fraction of twinned grains is now only 14% (Fig. 3b). The SEM micrograph of the same area (Fig. 3c) reveals that in the pure Mg polycrystal with $d = 5$ μm strain tends to concentrate along deformation slip bands making an angle with the compressive axis. These bands can be clearly seen in the corresponding post-straining EBSD map (Fig. 3b) as non-indexed points. Further details about slip bands are provided by the SEM micrographs at different magnifications of Fig. 3d–h. In areas relatively far from the deformation band propagation front (Fig. 3d–f), the first few slip traces start to appear and to transfer to neighboring grains. Within the deformation bands a large concentration slip traces are present (Fig. 3g and h). Again, an exhaustive EBSD-assisted analysis of 139 slip traces contained within the bands revealed that 73% corresponded to basal slip, 13% to prismatic ⟨a⟩ slip, and 14% to pyramidal ⟨c+a⟩ slip. Fig. 3i reveals that the SF for basal slip (SF_{basal})